Investigation of turbulent channel flow using local mesh refinement

Péter Füle, *Zoltán* Hernádi

Abstract

Large eddy simulation of turbulent channel flow is carried out at Re_τ values of 150 and 395. Mesh refinement effects are evaluated on conventional meshes, then local mesh refinement in streamwise direction is applied and investigated. The goal of the paper is to give proposal about the ideal position of the merging face and to show how many cells can be saved in this case without losing too much accuracy at both Reynolds numbers. The results are compared to DNS data.

Keywords

large eddy simulation · channel flow · local mesh refinement

Péter Füle

Departmet of Fluid Mechanics,
Budapest University of Technology and Economics
Bertalan Lajos street 4-6., H-1111 Budapest, Hungary
e-mail: fulepeter88@gmail.com

Zoltán Hernádi

Departmet of Fluid Mechanics,
Budapest University of Technology and Economics
Bertalan Lajos street 4-6., H-1111 Budapest, Hungary
e-mail: hernadi@ara.bme.hu

1 Introduction

Channel flows are important reference cases of LES development, e.g. investigating different grid structures or developing new sub-grid scale models [12,13]. In finite-volume simulations of turbulent channel flows it is very important to obtain the results in relatively short time and with acceptable accuracy. The computational costs of a simulation can be decreased by using lower amount of cells, but this way the accuracy is also decreased. Grid resolution in LES also determines which scales of eddies can be resolved, thus in a channel flow it is acceptable to use a lower streamwise resolution near the centerline, where larger eddies are present.

In the literature two main techniques of local mesh refinement can be found. One technique is to use embedded or nested grids where a finer resolution grid is embedded (nested) into a zone of the coarser grid (e.g. near the wall in channels). This type of mesh refinement is used in [9,2], and [11]. Using this technique, the interaction of meshes must be ensured which can make these simulations more complicated.

Another technique involves a single mesh for the whole simulation domain and in one direction the resolution can be non-homogeneous. In this case the mesh zones are in direct interaction and the transition is ensured by some prism or distorted hexahedron cells. These kinds of meshes are used in [8,7] and [1].

Various simulation approaches using local mesh refinement are in very good agreement with the corresponding DNS or experimental data for both external and internal flows.

The goal of this paper is to simulate a turbulent channel flow using large eddy simulation, to investigate the effects of decreasing streamwise resolution above a certain distance from the wall and to give proposals about the ideal region size of refinement and the reduction of resolution. The simulations are performed at $Re_\tau = 150$ and 395 to investigate the Reynolds number dependency of the results.

In the second section the methodology of the investigation is described. The governing equations of LES and the turbulent model are shown and shortly introduced along with the setup of the simulations. The third section describes the results

of the investigations. This section is separated into two sub-sections, which are the conventional meshes and the locally refined meshes. Using a step-by-step investigation a final, best performing mesh is obtained for both Reynolds numbers, then using these meshes the effects of local refinement in stream-wise direction are investigated. In the fourth section the conclusions of the investigations are described.

2 Methodology

2.1 Large Eddy Simulation

LES is a widely used method for simulating fluid flows with important turbulent structures. In contrast to Reynolds Averaged Navier-Stokes (RANS) methods that do not resolve turbulent eddies, LES is capable of resolving a part of the turbulent kinetic energy spectrum. The remaining part of the spectrum needs to be modelled. Figure 1 shows the difference in the resolved and modelled turbulent kinetic energy spectrum for RANS methods and LES [14].

The governing equations are the continuity equation (1) and the Navier-Stokes equations (2). These are filtered equations with an added SGS viscosity.

$$\frac{\partial \overline{u}_i}{\partial x_i} = 0 \tag{1}$$

$$\frac{\partial \overline{u}_i}{\partial t} + \frac{\partial}{\partial x_j}\left(\overline{u}_i \overline{u}_j\right) = -\frac{\partial \overline{p}}{\partial x_i} + \frac{\partial}{\partial x_j}\left[\left(v + v_{SGS}\right)\frac{\partial \overline{u}_i}{\partial x_j}\right] \tag{2}$$

Dynamic Smagorinsky model is used to model the SGS viscosity. The classical Smagorinsky model describes the sub-grid (modelled) viscosity using a constant number, the Smagorinsky constant [15].

$$v_{SGS} = \left(C_s \Delta\right)^2 \left|S_{ij}\right| \tag{3}$$

The dynamic Smagorinsky model calculates the value of the Smagorinsky constant in every time step locally for every cell. In order to perform this calculation a test grid is applied on which the filter width is wider than on the original grid (e.g. $\Delta_{test} = 2\Delta$) and the method of least squares is used [4,10].

The simulations are carried out using LES with the described dynamic Smagorinsky model in OpenFOAM, an open source C++ library using the built-in solver for channel flows with LES named channelFoam [17,6].

2.2 Simulation setup

Cyclic boundary condition is applied at every face except the walls. No-slip condition for the velocity field and zero-gradient for the pressure field is applied on the walls. A perturbed velocity field is used for initial condition [16, pp. 163-167].

The friction and bulk Reynolds numbers and mean velocities used are shown in Table 1. In the simulations Re_m has a prescribed value and Re_τ is a result of the simulation.
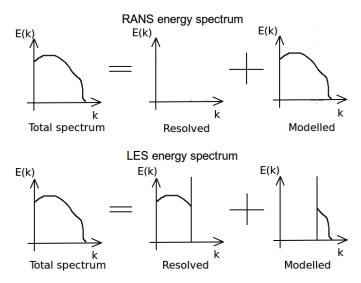

Fig. 1. RANS and LES energy spectra

Tab. 1. studied Reynolds numbers and velocities

Re_τ [-]	u_τ [m/s]	Re_m [-]	u_m [m/s]
150	0.0030	4586	0.004586
395	0.0079	13925	0.013925

The constant time step is set to maintain a CFL of 0.6 - 0.8 for the conventional meshes. Locally refined meshes has the same step size as their base conventional mesh. The effects of the local refinement on the CFL can be investigated this way. The results can be seen in section 3.2.

2.3 Geometry

Channel flow is a fluid flow between two infinitely large flat plates. The simulation domain is 4x2x2 meters ($L_x x L_y x L_z$). The used geometry is shown in Figure 2, where grey colour represents the channel walls and the others are cyclic faces.

2.4 Meshing techniques

Two meshing techniques are used during the investigations. First technique is used with conventional meshes: the resolution is changed in only one direction and the resolution is homogeneous for every direction. Mesh structure is shown in Figure 3.

Another technique is used with locally refined meshes. The resolution in streamwise direction is not homogeneous, but it is decreased above a certain distance from the channel wall. The structure of this kind of mesh is shown in Figure 4.

Cell size in wall normal direction is changing according to a geometric series. The quotient of the series is kept at 1.1 for every mesh.
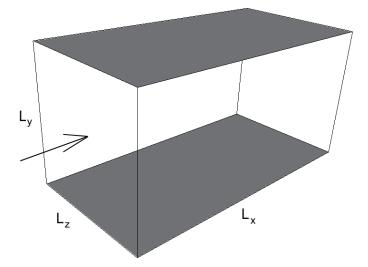
Fig. 2. Geometry of the channel: rectangular fluid domain with two parallel solid walls and cyclic faces in the homogeneous directions (x and z directions)

3 Results

Two main parameters are used to evaluate the results of the meshes. First is the relative difference of the friction Reynolds number (Eq. (4)) compared to the reference, the second is the normalized mean square error, which is calculated as Eq. (5). In our results NMSE is applied to the dimensionless streamwise mean velocity, $u^+=u/u_\tau$.

$$Re_\tau = \frac{u_\tau \delta}{v} \quad (4)$$

$$NMSE = \frac{\frac{1}{n}\sum_{i=1}^{n}\left(\hat{u}_i^+ - u_i^+\right)^2}{\frac{1}{n}\sum_{i=1}^{n}\hat{u}_i^+ u_i^+} \quad (5)$$

The reference values of Re_τ and u^+ are taken from DNS database [5].

3.1 Conventional meshes

Conventional meshes refer to homogeneous resolution in the main directions. Figure 3 shows this mesh structure.

According to [3] the suggested minimal resolution for LES is $\Delta x^+=100$, $y^+=1$ and $\Delta z^+=30$. Starting from this resolution at $Re_\tau=150$ a step-by-step investigation is carried out in order to reach mesh independent results. In every step the resolution is changed only in one direction. One mesh is considered better from another if the error of Re_τ and the NMSE also decrease. Table 2 and Table 3 show the investigation steps and results at $Re_\tau=150$.

The last row of Table 2 represents an intermediate state. Around this resolution other investigations are made, these steps are shown in Table 3, where the last row represents the final, best performing mesh.
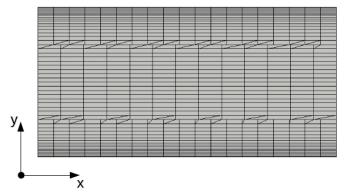

Fig. 3. Conventional mesh structure

Fig. 4. Locally refined mesh. Resolution near the wall is the same as in Figure 3, while the streamwise resolution near the centerline is almost 1.5 times coarser. Near wall and centerline blocks are merged by inserting prism cells at the merged faces.

Tab. 2. Results of conventional mesh investigation steps, first study, $Re_\tau=150$

Δx^+	y^+	Δz^+	error of Re_τ	NMSE
100	**1**	**30**	**34%**	**0.2526**
25	1	30	12%	0.0226
50	1	30	16%	0.0369
150	1	30	42%	0.4505
200	1	30	42%	0.4487
100	0.25	30	20%	0.0778
100	0.5	30	42%	0.4355
100	1.5	30	22%	0.0879
100	2	30	20%	0.0707
100	1	10	34%	0.2285
100	1	15	6%	0.0063
100	1	40	31%	0.2013
100	1	60	30%	0.1732
25	**2**	**15**	**6%**	**0.0053**

The results of the best performing mesh in Table 3 are in good agreement with the reference considering Re_τ error, which is 3%. The 10^{-4} order of magnitude of the NMSE is a reasonably good result too, especially when taking the total number of cells into consideration, which is 57000 cells. In contrast the reference DNS grid has more than 1.5 million cells at the same Re_τ [5].

Table 4 shows the investigation steps and results for Re_τ=395 and the last row represents the best performing mesh.

Results of the best performing mesh in Table 4 show that the error of Re_τ is 1% and the order of magnitude of the NMSE is 10^{-4}. The total number of cells is 195920 (the DNS reference has almost 9.5 million cells). The resolved part of the turbulent kinetic energy is above 90% for both Reynolds numbers.

In Figure 7 - Figure 10 "base mesh" legend represents the velocity and RMS profiles for these meshes.

Summarizing the results the minimal required resolution in our implementation can be described as Eq. (6)-(8).

$$\Delta x^+ \leq 32\dots40 \quad (6)$$

$$y^+ \leq 1\dots1.5 \quad (7)$$

$$\Delta z^+ \leq 5\dots10 \quad (8)$$

3.2 Locally refined meshes

Locally refined meshes refer to meshes, where the streamwise resolution is decreased above a certain distance from the channel walls. Figure 4 shows a locally refined mesh.

To perform the investigation of the effects of local mesh refinement, the final, best performing meshes of the conventional refinements are used. The resolution of the base mesh at Re_τ=150 is: Δx^+=32, y^+=1, Δz^+=5. At Re_τ=395 it is: Δx^+=40, y^+=1.5, Δz^+=10.

The two varied parameters during the local mesh refinement study are the wall-normal size of refined region (y_{MF}^+) and the streamwise resolution near the centerline (Δx_c^+). For Re_τ=150 the value of y_{MF}^+ is varied between 10…75 and Δx_c^+ is varied between 35…50. For Re_τ=395 the following ranges are studied: y_{MF}^+=55…95 and Δx_c^+=53…79. In this interval the relative error of the friction Reynolds number remains between ±5%.

Table 5 and Table 6 show the worst and the best results along with the parameters of the base meshes.

Table 5 and Table 6 show that 13-17% of the cells can be saved without significantly reducing accuracy (compared to the base mesh). At Re_τ=150 the maximum CFL is roughly 6% lower than on the base mesh, thus the time step can be somewhat higher. At Re_τ=395 the maximum CFL does not change significantly on the locally refined meshes compared to the base mesh.

Figure 5 and Figure 6 show tendencies of NMSE results on the investigated interval of the varied parameters. In the figures the two lines represent two typical values for both cases, i.e.

Tab. 3. Results of conventional mesh investigation steps, second study, Re_τ=150

Δx^+	y^+	Δz^+	error of Re_τ	NMSE
25	**2**	**15**	**6%**	**0.0053**
10	2	15	7%	0.0062
17	2	15	6%	0.0055
32	2	15	5%	0.0036
40	2	15	7%	0.0069
10	1	15	5%	0.0042
10	1.5	15	8%	0.0092
10	2.5	15	6%	0.0043
10	3	15	7%	0.0062
10	2	5	0%	0.0001
10	2	10	3%	0.0017
10	2	20	12%	0.0211
10	2	25	14%	0.0309
32	**1.5**	**5**	**3%**	**0.0008**

Tab. 4. Results of conventional mesh investigation steps, Re_τ=395

Δx^+	y^+	Δz^+	error of Re_τ	NMSE
25	**2**	**15**	**2%**	**0.00105**
10	2	15	5%	0.00357
17	2	15	5%	0.00357
32	2	15	3%	0.00177
40	2	15	1%	0.00081
10	1	15	3%	0.00135
10	1.5	15	2%	0.00090
10	2.5	15	3%	0.00093
10	3	15	3%	0.00089
10	2	5	3%	0.00046
10	2	10	1%	0.00005
10	2	20	5%	0.00414
10	2	25	8%	0.00863
40	**1.5**	**10**	**1%**	**0.00036**

one close to the wall and one far from the wall. The tendencies between these parameters are similar.

The farther the position of the merging face is from the channel walls, the better the results become for every investigated Δx_c^+ at both Reynolds numbers. According to Figure 5, decreasing the streamwise resolution near the centerline has a significant effect on the results at Re_τ=150 if y_{MF}^+ is low, i.e. the merging face is close to the wall, but has almost no effect if y_{MF}^+ is high enough. In case of Re_τ=395 decreasing Δx_c^+ also affects the NMSE results even if y_{MF}^+ is higher.

In the case of Re_τ=150 the best result is achieved by placing the merging face around y_{MF}^+=75. In wall normal distance this is equal to y=0.5·δ. In this case the streamwise resolution can be decreased by 47%. In the case of Re_τ=395 the best

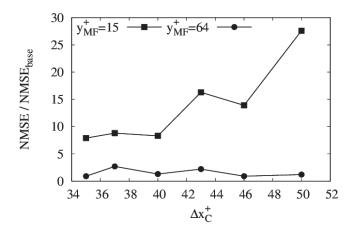**Fig. 5.** NMSE results normalized by the NMSE of the base mesh for two typical y_{MF}^+ values. Re_τ=150.
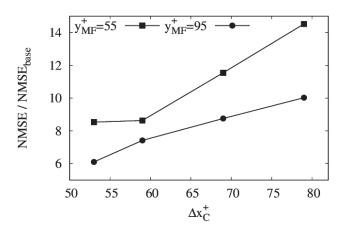

Fig. 8. Streamwise dimensionless mean velocity profiles, Re_τ=395.

Fig. 6. NMSE results normalized by the NMSE of the base mesh for two typical y_{MF}^+ values. Re_τ=395.

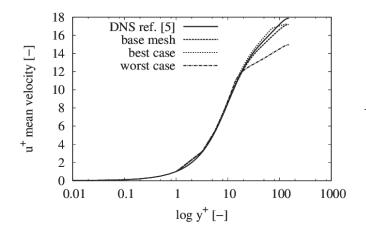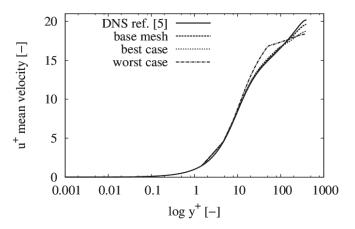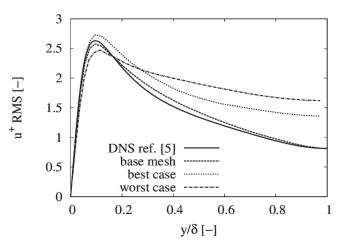**Fig. 9.** Streamwise dimensionless RMS velocity profiles, Re_τ=150.

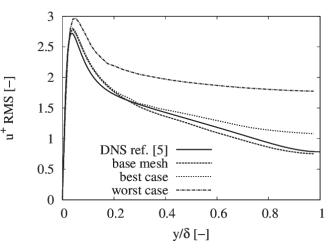**Fig. 7.** Streamwise dimensionless mean velocity profiles, Re_τ=150.

Fig. 10. Streamwise dimensionless RMS velocity profiles, Re_τ=395.

position of the merging face is around y^+_{MF} =95, which means y=0.24·δ and the resolution in the near centerline region can be decreased by around 25%.

Figure 7-10 show profiles of the streamwise mean velocity and RMS. For the best meshes the profiles correspond fairly well with the base mesh as the streamwise resolution is decreased near the centerline.

4 Summary

Wall-resolved large eddy simulations using Δx^+=32…40, y^+=1…1.5, Δz^+=5…10 resolutions are performed for Re_τ= 150 and 395 with very good agreement with DNS databases in literature.

Locally refined meshing technique is proposed in order to maintain computational resources and accuracy. The investigation of locally refined meshes shows that acceptable results can be achieved in terms of NMSE and the error of Re_τ by decreasing the streamwise resolution above a certain value of wall distance. The resolution can be decreased by 25-47% without losing too much accuracy.

As the log-law region of the turbulent boundary layer is closer to the wall for higher Re_τ, more cells can be saved without loosing accuracy by moving the merging face closer to the wall. The results obtained for both Re_τ values are in good agreement with this theory. The ideal position of the merging face gets closer to the wall at a higher Re_τ as it was described in section 3.2.

In future, the proposed non-dimensional parameters of locally refined meshes should be tested for higher Reynolds numbers.

Tab. 5. Comparison of the base, best and worst cases, Re_τ=150

	base mesh	best case	worst case
Δx^+	32	32	32
Δx_c^+	32	60	50
y^+	1	1	1
y^+_{MF}	-	75	15
Δz^+	5	5	5
NMSE/NMSE$_{base}$	1	0.7	27.6
CFL$_{base}$/CFL	1	1.06	1.23
n^{saved}_{cells}	0%	17%	28%

Tab. 6. Comparison of the base, best and worst cases, Re_τ=395

	base mesh	best case	worst case
Δx^+	40	40	40
Δx_c^+	40	53	79
y^+	1.5	1.5	1.5
y^+_{MF}	-	95	55
Δz^+	10	10	10
NMSE/NMSE$_{base}$	1	6.1	14.5
CFL$_{base}$/CFL	1	1.00	1.05
n^{saved}_{cells}	0%	13%	32%

Nomenclature

Acronyms
DNS   Direct Numerical Simulation
LES   Large Eddy Simulation
RANS Reynolds Averaged Navier-Stokes
RMS   Root mean square
SGS   Sub-grid scales

Oversymbols
—   filtered value
^   simulated value

Greek symbols
Δ [m]   LES filter width
Δ_{test} [m]   test filter width
δ [m]   channel half width
v [m/s²]   molecular viscosity
v_{SGS} [m/s²]   sub-grid scale viscosity

Roman symbols
E [m²/s²]   turbulent kinetic energy
L_x [m]   channel streamwise length
L_y [m]   channel width (wall normal direction)
L_z [m]   channel spanwise length
k [1/m]   wavenumber
n^{saved}_{cells} [%]   cell number reduction in %
p [m²/s²]   pressure

s_{ij} [1/s]   symmetric component
                  of the velocity gradient tensor
t [s]   time
u_i [m/s]   i-th component of the velocity vector
u_m [m/s]   bulk velocity
u_τ [m/s]   friction velocity
x_i [-]   i-th direction
y [m]   wall normal distance

Dimensionless groups

CFL	[-]	Courant number
C_s	[-]	Smagorinsky constant
$NMSE$	[-]	normalized mean square error
Re_τ	[-]	friction Reynolds number
Re_m	[-]	bulk Reynolds number
u^+	[-]	dimensionless streamwise velocity

y^+	[-]	dimensionless wall normal distance
y_{MF}^+	[-]	position of the merging face
Δx^+	[-]	dimensionless streamwise resolution
Δx_c^+	[-]	dimensionless streamwise resolution near the channel centerline
Δz^+	[-]	dimensionless spanwise resolution

Acknowledgements

References

1 Aman V, Krishnan M, A *Lagrangian subgrid-scale model with dynamic estimation of Lagrangian time scale for large eddy simulation of complex flows*, Physics of Fluids 24 (8) (2012).
DOI: 10.1063/1.4737656

2 Boersma B. J., Kooper M. N., Nieuwstadt F. T. M., *Wesseling P., Local Grid Refinement in Large-Eddy Simulation*. Journal of Engineering Mathematics, 32 (2-3), 161-175 (1997).
DOI: 10.1023/A:1004283921077

3 Davidson L., *Fluid mechanics, turbulent flow and turbulence modeling*. Chalmers University of Technology, Göteborg, Sweden (2012).

4 Germano M., Piomelli U., Moin P., Cabot W. H., *A dynamic subgrid-scale eddy viscosity model*. Physics of Fluids A: Fluid Dynamics (1989-1993), 3 (7), 1760-1765 (1991).
DOI: 10.1063/1.857955

5 Iwamoto K., Suzuki Y., Kasagi N., *Reynolds number effect on wall turbulence: toward effective feedback control*. International Journal of Heat and Fluid Flow, 23 (5), 678-689 (2002)
DOI: 10.1016/S0142-727X(02)00164-9

6 Jasak H., *OpenFOAM: Open source CFD in research and industry*. International Journal of Naval Architecture and Ocean Engineering, 1 (2), 89-94 (2009).

7 Denev J. A., Fröhlich J., Bockhorn H, Schwertfirm F., Manhart M., *DNS and LES of Scalar Transport in a Turbulent Plane Channel Flow at Low Reynolds Number*. in 'Large-Scale Scientific Computing' (eds.: Lirkov I., Margenov S., Waśniewski J.) Springer Berlin Heidelberg, Vol 4818, 251–258 (2008).
DOI: 10.1007/978-3-540-78827-0_27

8 Kang S., Iaccarino G., Ham F., Moin P., *Prediction of wall-pressure fluctuation in turbulent flows with an immersed boundary method*. Journal of Computational Physics, 228 (18), 6753–6772 (2009).
DOI: 10.1016/j.jcp.2009.05.036

9 Kravchenko A. G., Moin P., Moser R., *Zonal Embedded Grids for Numerical Simulations of Wall-Bounded Turbulent Flows*. Journal of Computational Physics, 127 (2), 412-423 (1996).
DOI: 10.1006/jcph.1996.0184

10 Lilly D. K., *A proposed modification of the Germano subgrid-scale closure method*. Physics of Fluids A: Fluid Dynamics, 4 (3), 633–635 (1992).
DOI: 10.1063/1.858280

11 Ling L., Mingshun Y., Quanming L., *Zonal embedded grids for LES of self-sustaining structures of wall turbulence*. Tsinghua Science and Technology, 15 (5), 555-560 (2010).
DOI: 10.1016/S1007-0214(10)70100-0

12 Meyers J., Sagaut P., *Is plane-channel flow a friendly case for the testing of large-eddy simulation subgrid-scale models?* Physics of Fluids, 19 (4) (2007).
DOI: 10.1063/1.2722422

13 Meyers J., Sagaut P., *Evaluation of Smagorinsky variants in large-eddy simulations of wall-resolved plane channel flows*. Physics of Fluids, 19 (9) (2007).
DOI: 10.1063/1.2768944

14 Sagaut P., *Large Eddy Simulation for Incompressible Flows: An Introduction*, Third Edition, Springer, Germany (2006).

15 Smagorinsky J., *General Circulation Experiments with the Primitive Equations*. Monthly Weather Review, 91 (3), 99 – 164 (1963).
DOI: 10.1175/1520-0493(1963)091<0099:GCEWTP>2.3.CO;2

16 de Villiers E., *The Potential of Large Eddy Simulation for the Modeling of Wall Bounded Flows*. Imperial College of Science, Technology and Medicine (2006).

17 Weller H. G., Tabor G., Jasak H., Fureby C., *A tensorial approach to computational continuum mechanics using object-oriented techniques*. Computers in Physics, 12 (6), 620-631 (1998).
DOI: 10.1063/1.168744